

High $\text{NH}_2\text{D}/\text{NH}_3$ ratios in protostellar cores

J. Hatchell*

Max-Planck-Institut für Radioastronomie, Auf dem Hügel 69, 53121 Bonn, Germany

Received 20 June 2002 / Accepted 1 March 2003

Abstract. Observations of low mass protostars which probe small enough size scales to be within likely CO depletion regions show the highest $[\text{NH}_2\text{D}]/[\text{NH}_3]$ ratios yet measured, of 4–33%. These molecular D/H ratios are higher than those measured on larger scales, showing that deuterium fractionation increases towards protostellar cores. As in cold clouds, such high ratios can be produced by gas-phase ion-molecule chemistry in the presence of depletion. Grain surface chemistry is less likely to explain the deuterium enhancement, as it would require higher fractionation in ices than current models predict. The link between accretion, depletion and high molecular deuterium fractionation is strongly supported.

1. Introduction

There are two main ways of producing molecular D/H enhancements in molecular clouds over the $\sim 10^{-5}$ ratio of $[\text{HD}]/[\text{H}_2]$. Firstly, grain surface chemistry may enhance molecular D/H ratios (Brown & Millar 1989a, 1989b; Charnley et al. 1997). Secondly, some key gas phase reactions involving destruction of deuterated species run slower at low temperatures than the equivalent reactions with hydrogen, and this leads to molecular D/H enhancements where a cold gas phase chemistry has been active. Furthermore, in colder gas, depletion of heavy molecules such as CO results in an increase of $[\text{H}_2\text{D}^+]/[\text{H}_3^+]$ and molecular D/H ratios (Brown & Millar 1989a; Roberts & Millar 2000a, 2000b; Rodgers & Charnley 2001).

Depletion of heavy molecules during freezeout in cold molecular clouds can result in molecular D/H ratios above 10% (Roberts & Millar 2000), and can explain many of the high ratios observed in cold, dark clouds: DCO^+ fractionation in L1544 and L134N (Caselli et al. 1999; Tiné et al. 2000) and ND_2H in L134N (Roueff et al. 2000).

Young protostars should show the effect of freezeout as well as cold dark clouds, though grain mantle release may also influence the ratios, as in IRAS 16293–2422 (van Dishoeck et al. 1995). A few studies have looked at molecular D/H ratios in low mass protostars: HDCO and DCN (Roberts et al. 2002); NH_2D (Shah & Wootten 2001; Saito et al. 2000); DCO^+ (Williams et al. 1998). However, the 70–90'' beam size of most of these studies is a severe limitation as the largest D/H enhancements are expected on small scales, where densities are high. In L1544, heavy depletion occurs in a region 13 000 AU across – only 90'' diameter in nearby Taurus (Caselli et al. 1999). In order to prove a general link between accretion and high D/H ratios, observations are needed of molecular D/H ratios in a sample of protostars with high enough resolution to probe the depletion regions.

I present the results of such a survey of $[\text{NH}_2\text{D}]/[\text{NH}_3]$ ratios towards 11 protostars in Perseus, Taurus and Orion, observing NH_2D with the IRAM 30 m at 28'' resolution (maximally 11 000 AU at the distance of Orion) and centering the observations on the protostellar dust peaks where the strongest depletion is likely to be found.

2. Observations

NH_2D observations were made at the IRAM 30 m on Pico Veleta in May 2000 and June 2002 towards 11 protostellar objects in Perseus, Taurus and Orion (Table 1). I observed the 85.93 GHz $1(1, 1)–1(0, 1)$ ortho transitions (6 hyperfine lines) (see Olberg et al. 1985). The $1(1, 1)$ state lies 20.7 K above ground. Integration times were 10 min (position switched) and 20 min for the two Orion sources; system temperatures were 165–190 K with typical summer conditions of 4 mm PWV (precipitable water vapour). Observations of the two NGC 1333 sources in June 2002 were made under 7 mm PWV ($T_{\text{sys}} = 260–290$ K). Noise levels were 50–90 mK on 40 kHz channels. Spectra were corrected for the beam efficiency $B_{\text{eff}} = 0.73$.

The main NH_2D line was detected in all 11 sources. In the seven Perseus sources, the four outlying hyperfine transitions were also detected with peak brightness above 5σ . In L1551IRS5, the hyperfine transitions were above 3σ . In the other Taurus and Orion sources, only the main hyperfine line was detected. Spectra are shown in Fig. 1.

NH_3 observations at 24 GHz were made at the Effelsberg 100 m in May 2002 using the 8192-channel spectrometer, which allows observation of the $(J, K) = (1, 1)–(4, 4)$ metastable transitions simultaneously. System temperatures were 40–50 K. Calibration was checked on W3(OH) and spectra were converted to Kelvin. The Effelsberg beamsize at 24 GHz is 37''. $\text{NH}_3(1, 1)$ was detected in all sources; the $\text{NH}_3(1, 1)$ hyperfines and the $(2, 2)$ main line were detected in

* e-mail: hatchell@mpi-fr-bonn.mpg.de

Table 1. Source positions and velocities.

Object	RA (J2000) [h m s]	Dec (J2000) [° ' "]	v_{LSR} km s ⁻¹
<i>Perseus</i>			
B5IRS1	03 47 41.3	+32 51 42	10.2
L1448mms	03 25 38.8	+30 44 05	4.7
L1448NW	03 25 35.6	+30 45 34	4.7
HH211	03 43 56.8	+32 00 50	9.2
IRAS 03282+3035	03 31 20.4	+30 45 25	7.1
NGC 1333 IRAS 4A	03 26 04.8	+31 03 14	7.0
NGC 1333 DCO ⁺	03 26 06.6	+31 03 08	6.5
<i>Taurus</i>			
L1551IRS	04 31 34.1	+18 08 05	6.2
L1527	04 39 53.5	+26 03 05	5.7
<i>Orion</i>			
RNO43	05 32 19.4	+12 49 32	10.4
HH111	05 51 46.3	+02 48 30	8.5

all sources except the two Orion sources (RNO43 and HH111). The upper state energies for the (1, 1) and (2, 2) lines are 23.8 and 65.0 K respectively. The (3, 3) and (4, 4) lines were not detected.

3. Analysis and results

NH_2D observations for the Perseus sources with well-detected hyperfines were reduced using CLASS method HFS to fit the six hyperfine lines (see Tiné et al. 2000 for frequencies and line strengths) and derive optical depths and linewidths (Table 2). Where not all the hyperfines were detected, or the HFS fit gave too great an uncertainty in the optical depth, the main line was fitted with a single Gaussian (L1527, L1551IRS5, RNO43, HH111).

$\text{NH}_3(1, 1)$ observations were reduced using CLASS method $\text{NH}_3(1, 1)$ to fit the hyperfine structure and derive optical depths and linewidths (Table 2). Excitation temperatures in the (1, 1) line were 5–10 K assuming unity filling factor, but as the filling factor is uncertain these temperature estimates are of limited value. More usefully, I derived the rotation temperature T_{12} using the method of Bachiller et al. (1987), fitting the (2, 2) main line with a single Gaussian. These temperatures are independent of filling factor and calibration. Rotation temperatures were $T_{12} = 11$ –14 K in the Taurus and Perseus sources. At these low temperatures, the rotational temperature is a good approximation to the kinetic temperature $T_{12} \approx T_{\text{kin}}$ (Walmsley & Ungerechts 1983). For RNO43 in Orion, $T_{12} = 14.6$ K. The $\text{NH}_3(2, 2)$ line in the other Orion source, HH111, was too weak for an estimate of T_{12} .

For the Perseus sources, optical depths were available from hyperfine fits, and column densities and $[\text{NH}_2\text{D}]/[\text{NH}_3]$ ratios were derived assuming LTE at $T_{\text{kin}} = T_{12}$. The resulting $[\text{NH}_2\text{D}]/[\text{NH}_3]$ ratios are 0.17–0.33 (Table 3).

For the Taurus sources L1527 and L1551 IRS5, optical depths were available for NH_3 but not for NH_2D . NH_2D beam-averaged column densities were derived from the main hyperfine integrated intensities at $T_{\text{kin}} = T_{12}$. The low

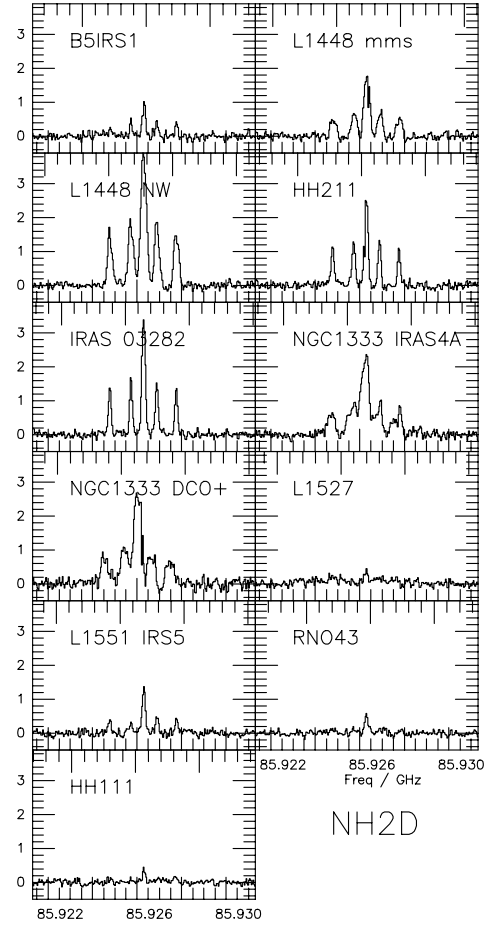


Fig. 1. NH_2D (upper) and NH_3 (lower) spectra. The temperature scale is T_{MB} in Kelvin. Note that the NH_2D lines appear wider because of the factor 3.6 frequency difference between the NH_3 and NH_2D transitions.

$[\text{NH}_2\text{D}]/[\text{NH}_3]$ ratios, 0.04–0.05, likely reflect the fact that the NH_2D column densities are beam-averaged whereas the NH_3 optical depths refer to higher column density material on smaller scales, so the ratios are lower limits.

For the Orion sources RNO43 and HH111, $\text{NH}_3(1, 1)$ optical depths were much less than one and very uncertain, so the NH_3 beam averaged column density was calculated from the integrated intensity of the main hyperfine line. NH_2D and NH_3 column densities were calculated at 14.6 K (the measured T_{12} in RNO43). The ratios are additionally divided by the ratio of the beam areas to give $[\text{NH}_2\text{D}]/[\text{NH}_3]$ ratios of 11–22%. This assumes that the source is centrally condensed and $N(\text{NH}_3)$ is higher on the NH_2D beam scales. The correction is conservative, and the $[\text{NH}_2\text{D}]/[\text{NH}_3]$ ratios for the Orion sources could be a factor of 1.75 higher if the NH_2D is extended, or 19–39%.

When calculated without optical depth information the ratios are less certain, as the absolute calibration uncertainty at each frequency is $\sim 30\%$. In contrast, where optical depths are measured the $[\text{NH}_2\text{D}]/[\text{NH}_3]$ ratio does not depend on the absolute calibration. All the column density determinations are of course limited by the lack of information about source structure from single spectra. Foreground self-absorption and multiple components (which particularly affect NGC 1333) and the

Table 2. NH₂D and NH₃ observed line parameters. Uncertainties (in brackets) come from either formal errors on optical depth from the hyperfine fits or 30% absolute calibration uncertainties where column density was derived from integrated intensity.

Source	NH ₂ D 85.93 GHz				NH ₃ (1, 1)		NH ₃ (2, 2)
	τ	$\int T_{\text{MB}}^* dv$ K km s ⁻¹	Δv km s ⁻¹	τ	$\int T_{\text{MB}}^* dv$ K km s ⁻¹	Δv km s ⁻¹	$\int T_{\text{MB}}^* dv$ K km s ⁻¹
B5IRS1	3.22 (0.74)	–	0.46 (0.03)	3.74 (0.06)	–	0.58 (0.00)	0.27 (0.02)
L1448mms	2.43 (0.29)	–	0.88 (0.02)	2.79 (0.04)	–	1.00 (0.00)	1.23 (0.05)
L1448NW	3.66 (0.12)	–	0.83 (0.01)	5.37 (0.04)	–	0.89 (0.00)	1.41 (0.03)
HH211	4.54 (0.28)	–	0.49 (0.01)	2.70 (0.15)	–	0.68 (0.01)	0.53 (0.03)
IRAS 03282	3.39 (0.18)	–	0.50 (0.01)	3.53 (0.15)	–	0.59 (0.01)	0.39 (0.02)
NGC 1333 IRAS 4A	1.46 (0.29)	–	1.38 (0.04)	1.66 (0.50)	–	1.28 (0.06)	0.78 (0.15)
NGC 1333 DCO ⁺	1.84 (0.25)	–	1.19 (0.02)	2.54 (0.08)	–	1.20 (0.01)	0.95 (0.04)
L1527	–	0.247 (0.074)	0.83 (0.13)	1.51 (0.01)	–	0.50 (0.01)	0.15 (0.02)
L1551IRS5	–	0.680 (0.204)	0.60 (0.03)	2.14 (0.02)	–	0.66 (0.01)	0.52 (0.03)
RNO43	–	0.301 (0.090)	0.68 (0.07)	–	0.791 (0.237)	1.04 (0.04)	0.18 (0.02)
HH111	–	0.177 (0.053)	0.51 (0.07)	–	0.964 (0.289)	1.03 (0.04)	–

Table 3. Temperatures, column densities and [NH₂D]/[NH₃] ratio.

Source	T_{12} K	$N(\text{NH}_2\text{D})$ $\times 10^{14}$ cm ⁻²	$N(\text{NH}_3)$ $\times 10^{14}$ cm ⁻²	[NH ₂ D]/ [NH ₃]
B5IRS1	10.8	2.12(0.49)	13.4(0.2)	0.18(0.04)
L1448mms	13.7	3.95(0.47)	18.0(0.3)	0.20(0.02)
L1448NW	11.7	4.74(0.16)	29.7(0.2)	0.17(0.01)
HH211	12.8	3.85(0.24)	11.6(0.6)	0.33(0.03)
IRAS 03282	11.3	2.52(0.13)	12.9(0.6)	0.22(0.01)
NGC 1333:				
IRAS 4A	14.2	3.90(0.78)	13.8(4.2)	0.25(0.09)
DCO ⁺	12.8	3.76(0.51)	19.2(0.6)	0.19(0.03)
L1527	10.8	0.16(0.05)	3.79(0.02)	0.04(0.02)
L1551IRS5	12.6	0.42(0.12)	8.88(0.07)	0.05(0.01)
RNO43	14.6	0.18(0.05)	0.46(0.14)	0.22(0.10)
HH111	–	0.10(0.03)	0.56(0.17)	0.11(0.06)

beam size difference between Effelsberg and the 30 m cannot be fully accounted for with the present data.

4. Discussion

In the Perseus sources where the ratios are best determined, [NH₂D]/[NH₃] = 17–33%. The highest ratios derived by Shah & Wootten (2001) and Saito et al. (2000) are 13% for sources also on this sourcelist. Differences in excitation assumptions may also have an effect, but the lower ratios derived by Shah & Wootten (2001) can easily be explained if the fractionation is enhanced on small scales, towards the protostellar cores, as their beam is larger (80–90'' compared to 27''). Saito et al. (2000)'s 18'' resolution observation towards B1 is 15'' away from the dust peak (Matthews & Wilson 2002) and shows a lower ratio, which also supports the idea that [NH₂D]/[NH₃] reduces away from the cores. (No conclusion can be drawn from their uncertain NH₂D column in L1448.) The ratios for protostars are also higher than those towards L134N, presumably because the protostars are denser and more depleted ([NH₂D]/[NH₃] = 0.1; Tiné et al. 2000).

Why should [NH₂D]/[NH₃] be higher close to the protostars? Is cold gas-phase chemistry in the presence of freezeout enhancing ratios in the cores, or are highly fractionated grain ices evaporating near the young stars?

Chemical models indicate that [NH₂D]/[NH₃] ratios of 30% can be produced by ion-molecule chemistry if heavy molecules are depleted (see Fig. 3 of Roberts & Millar 2000b; Fig. 2 of Rodgers & Charnley 2001). The ratios can be even higher if branching ratios for dissociative recombination favour deuterium retention (Lis et al. 2002). The corresponding fractionation required in molecular ions is similar or less than that already measured in L134N (Rodgers & Charnley 2001; N₂D⁺ observations by Tiné et al. 2000). Gas-phase chemistry with freezeout and depletion can therefore relatively easily explain the high [NH₂D]/[NH₃] ratios.

An alternative hypothesis is that removal of highly fractionated grain mantles enhances ratios. Infrared observations suggest that NH₃ may be present in ices, though the level is still uncertain (Lacy et al. 1998; Gibb et al. 2000; Dartois & D'Hendecourt 2001), but NH₃ ice alone evaporates at 60–70 K; in a water matrix temperatures greater than 90 K are required. The temperatures of our sources, which are mostly Class 0 protostars, rule out much thermal ice evaporation. Only B5IRS1 and L1551 have bolometric (dust) temperatures above 60 K. The source with the highest [NH₂D]/[NH₃] ratio, HH211, is probably extremely young (Gueth & Guilloteau 1999) and has a bolometric temperature of only 30 K. Kinetic temperature estimates for the NH₃ are all less than 15 K.

The possibility remains that highly fractionated grain mantles are being removed by non-thermal evaporation, ie. slow, non-dissociative shocks. [NH₂D]/[NH₃] ratios are around 10% in regions where grain evaporation is known to be occurring (hot cores and IRAS 16293; van Dishoeck et al. 1995), and may originate in the ices, as may high [D₂CO]/[H₂CO] ratios (Ceccarelli et al. 1998, 2002). Enhancements of another molecule, CH₃OH, in a similar sample of cores, are also attributed to non-thermal ice evaporation (Buckle & Fuller 2002). Two conditions must be satisfied if a non-thermal removal mechanism operates. Firstly, it must reproduce the

low linewidths of the NH_3 ($<1 \text{ km s}^{-1}$) and NH_2D (linewidths the same or lower), which suggest that NH_2D is tracing quiescent rather than shocked material. Secondly, if the release of ice material is to explain all the NH_2D observed, the $[\text{NH}_2\text{D}]/[\text{NH}_3]$ ratio in the ices must be as high or higher than that measured in the gas phase, because of dilution by low $[\text{NH}_2\text{D}]/[\text{NH}_3]$ ratios in regions of the core without ice evaporation.

Observations suggest that, in these sources, ices can only be released in a small fraction of the core, otherwise CH_3OH enhancements of several hundred percent would be expected, as seen in outflows and hot cores, rather than the moderate 10% observed (Buckle & Fuller 2002), and column densities of NH_3 would be enhanced by orders of magnitude over the surrounding molecular clouds, which is not the case (Bachiller et al. 1987, 1991, 1993; Benson & Myers 1989; Anglada et al. 1989).

To obtain the observed ratios even without dilution, the statistical treatment of Rodgers & Charnley (2001) following Brown & Millar (1989a, 1989b) requires an atomic D/H ratio in the gas phase at the time of freezeout of 0.8–1.6. This is at the limit of what either steady-state or depletion models predict, as these cannot produce atomic D/H > 0.1 (Roberts & Millar 2000a; Roberts, priv. comm.).

With dilution, therefore, current theories of grain mantle chemistry cannot explain the NH_2D enhancement, but would require either higher $[\text{D}]/[\text{H}]$ ratios during freezeout or preferential formation of deuterated molecules in the ice.

The $[\text{NH}_2\text{D}]/[\text{NH}_3]$ ratios of ~ 0.2 in NGC 1333 is consistent with ND_3 column densities (van der Tak et al. 2002; Lis et al. 2002), using the models of Rodgers & Charnley (2001). This is in contrast to earlier $[\text{NH}_2\text{D}]/[\text{NH}_3]$ ratios of 10% which predicted $[\text{ND}_3]/[\text{NH}_3]$ an order of magnitude lower than measured. As the theory predicts $[\text{ND}_3]/[\text{NH}_3] \propto [\text{NH}_2\text{D}]/[\text{NH}_3]^3$, ND_3 predictions are very sensitive to $[\text{NH}_2\text{D}]/[\text{NH}_3]$ ratios, and more observations of both isotopomers are needed to say if the theories for multiple deuteration are correct. Measurements of ND_2H in the same sources would provide a further test: $[\text{ND}_2\text{H}]/[\text{NH}_3] \sim 0.03$ is expected from the models, for the given $[\text{NH}_2\text{D}]/[\text{NH}_3]$ ratios. Detailed maps of individual sources would also test the relationship between high deuteration and CO depletion.

5. Summary and conclusion

$[\text{NH}_2\text{D}]/[\text{NH}_3]$ ratios in low mass protostellar cores on 10 000 AU scales can reach 30% percent. Such high ratios can be simply explained by recent models of cold gas-phase chemistry with depletion due to freezeout (Roberts & Millar 2000a, 2000b). Current models of ice formation even under conditions

of high depletion have difficulty explaining the high fractionation observed.

Acknowledgements. The author would like to thank Malcolm Walmsley, Floris van der Tak and Helen Roberts for useful discussions. This work was supported by the Deutsche Forschungsgemeinschaft SFB 494.

References

- Anglada, G., Rodriguez, L. F., Torrelles, J. M., et al. 1989, *ApJ*, 341, 208
- Bachiller, R., Guilloteau, S., & Kahane, C. 1987, *A&A*, 173, 324
- Bachiller, R., Martín-Pintado, J., & Planesas, P. 1991, *A&A*, 251, 639
- Bachiller, R., Martín-Pintado, J., & Fuente, A. 1993, *ApJ*, 417, L45
- Benson, P. J., & Myers, P. C. 1989, *ApJS*, 71, 89
- Brown, P. D., & Millar, T. J. 1989a, *MNRAS*, 237, 661
- Brown, P. D., & Millar, T. J. 1989b, *MNRAS*, 240, 25
- Buckle, J. V., & Fuller, G. A. 2002, *A&A*, 381, 77
- Caselli, P., Walmsley, C. M., Tafalla, M., Dore, L., & Myers, P. C. 1999, *ApJ*, 523, L165
- Ceccarelli, C., Castets, A., Loinard, L., Caux, E., & Tielens, A. G. G. M. 1998, *A&A*, 338, 43
- Ceccarelli, C., Vastel, C., Tielens, A. G. G. M., et al. 2002, *A&A*, 381, L17
- Charnley, S. B., Tielens, A. G. G. M., & Rodgers, S. D. 1997, *ApJ*, 482, L203
- Dartois, E., & D'Hendecourt, L. 2001, *A&A*, 365, 144
- Gibb, E. L., Whittet, D. C. B., Schutte, W. A., et al. 2000, *ApJ*, 536, 347
- Gueth, F., & Guilloteau, S. 1999, *A&A*, 343, 571
- Lacy, J. H., Faraji, H., Sandford, S. A., & Allamandola, L. J. 1998, *ApJ*, 501, L105
- Lis, D. C., Roueff, E., Gerin, M., et al. 2002, *ApJ*, 571, L55
- Matthews, B. C., & Wilson, C. D. 2002, *ApJ*, 574, 822
- Roberts, H., & Millar, T. J. 2000, *A&A*, 361, 388
- Roberts, H., & Millar, T. J. 2000, *A&A*, 364, 780
- Roberts, H., Fuller, G. A., Millar, T. J., Hatchell, J., & Buckle, J. V. 2002, *A&A*, 381, 1026
- Rodgers, S. D., & Charnley, S. B. 2001, *ApJ*, 553, 613
- Roueff, E., Tiné, S., Coudert, L. H., et al. 2000, *A&A*, 354, L63
- Saito, S., Ozeki, H., Ohishi, M., & Yamamoto, S. 2000, *ApJ*, 535, 227
- Shah, R. Y., & Wootten, A. 2001, *ApJ*, 554, 933
- Tiné, S., Roueff, E., Falgarone, E., Gerin, M., & Pineau des Forêts, G. 2000, *A&A*, 356, 1039
- van der Tak, F. F. S., Schilke, P., Müller, H. S. P., et al. 2002, *A&A*, 388, L53
- van Dishoeck, E. F., Blake, G. A., Jansen, D. J., & Groesbeck, T. D. 1995, *ApJ*, 447, 760
- Walmsley, C. M., & Ungerechts, H. 1983, *A&A*, 122, 164
- Williams, J. P., Bergin, E. A., Caselli, P., Myers, P. C., & Plume, R. 1998, *ApJ*, 503, 689